JOURNAL OF VIROLOGY, June 2005, p. 7528–7534 Vol. 79, No. 12
0022-538X/05/$08.00+0 doi:10.1128/JVI.79.12.7528–7534.2005

Invasion of the Central Nervous System in a Porcine Host by Nipah Virus

Hana Weingartl,[1,2]* Stefanie Czub,[1] John Copps,[1] Yohannes Berhane,[1] Deborah Middleton,[3] Peter Marszal,[1] Jason Gren,[1] Greg Smith,[1] Shelley Ganske,[1] Lisa Manning,[1] and Markus Czub[2,4]

National Centre for Foreign Animal Disease, Canadian Food Inspection Agency, Canadian Science Centre for Human and Animal Health, Winnipeg, Canada[1]; Australian Animal Health Laboratory, CSIRO, Geelong, Australia[3]; National Microbiology Laboratory, Public Health Agency of Canada, Canadian Science Centre for Human and Animal Health, Winnipeg, Canada[4]; and Department of Medical Microbiology, Faculty of Medicine, University of Manitoba, Winnipeg, Canada[2]

Received 23 November 2004/Accepted 1 March 2005

Nipah virus, a newly emerged zoonotic paramyxovirus, infects a number of species. Human infections were linked to direct contact with pigs, specifically with their body fluids. Clinical signs in human cases indicated primarily involvement of the central nervous system, while in pigs the respiratory system was considered the primary virus target, with only rare involvement of the central nervous system. Eleven 5-week-old piglets were infected intranasally, orally, and ocularly with 2.5×10^5 PFU of Nipah virus per animal and euthanized between 3 and 8 days postinoculation. Nipah virus caused neurological signs in two out of eleven inoculated pigs. The rest of the pigs remained clinically healthy. Virus was detected in the respiratory system (turbinates, nasopharynx, trachea, bronchus, and lung in titers up to $10^{5.3}$ PFU/g) and in the lymphoreticular system (endothelial cells of blood and lymphatic vessels, submandibular and bronchiolar lymph nodes, tonsil, and spleen with titers up to 10^6 PFU/g). Virus presence was confirmed in the nervous system of both sick and apparently healthy animals (cranial nerves, trigeminal ganglion, brain, and cerebrospinal fluid, with titers up to $10^{7.7}$ PFU/g of tissue). Nipah virus distribution was confirmed by immunohistochemistry. The study presents novel findings indicating that Nipah virus invaded the central nervous system of the porcine host via cranial nerves as well as by crossing the blood-brain barrier after initial virus replication in the upper respiratory tract.

A previously unknown virus emerged in 1998 in Malaysia. The virus, isolated in 1999 from cerebrospinal fluid (CSF) of human fatal cases, was named Nipah virus (3, 15) and found to be antigenically and genomically related to Hendra virus, isolated in 1994 in Australia (16, 26). Following further studies, the two enveloped negative-strand RNA viruses, Hendra and Nipah, were classified into a distinct taxonomic unit (genus *Henipavirus*) within the family *Paramyxoviridae* (9, 21). Even though pigs are considered the amplifying host for the Nipah virus and the source of virus in human infections, the natural reservoir of the virus is likely fruit bats from the genus *Pteropus* (4).

During the outbreak in Malaysia, up to 15% of human infections were estimated to be asymptomatic. The mortality in clinical cases was around 40%, due to acute encephalitic syndrome, with signs suggesting involvement of the brain stem and of the upper cervical cord. Some of the patients (40%) presented with accompanying respiratory disease (3, 24).

The disease in pigs is called porcine respiratory and encephalitis syndrome. Although the infection rate is estimated to be 100%, a large percentage of the pigs remained asymptomatic. Pigs under the age of 6 months had primarily respiratory disease accompanied by a strong "barking-type" cough with only a few animals showing neurological signs. The majority (85 to 95%) of the diseased pigs recovered (15).

In the natural and experimental (oral or subcutaneous) infections of swine, viral antigen was detected by immunohistochemistry in tonsils (crypt epithelium, lymphoid cells), respiratory epithelium (tracheal, bronchial, bronchiolar, and alveolar), including intranasal epithelial cells, kidneys (glomeruli and interstitium), and lymph nodes, in the endothelial and smooth muscle cells of small blood vessels, endothelial cells of lymphatic vessels, in arachnoid cells of meninges, in some cells (likely astrocytes) across the glia limitans, and in the connective tissue surrounding the trigeminal ganglion (10, 14). Tanimura and colleagues (19) also detected Nipah virus antigen in the Schwann cells of the peripheral nerve fascicles of the spleen of naturally infected pigs.

The site of primary replication of the Nipah virus is not known. In humans, blood vessels appear to be one of the early targets, with viral antigen detected in the endothelium and tunica media. Necrotic plaques containing viral antigen in neurons and glial cells were found in the brain. The antigen was also detected in meninges near small blood vessels. The choroid plexus was negative for viral antigen, while the spinal cord showed positive staining for viral antigen. Lungs were the second most severely affected infected organ (4, 25).

* Corresponding author. Mailing address: National Centre for Foreign Animal Disease, Canadian Food Inspection Agency, Canadian Science Centre for Human and Animal Health, 1015 Arlington St., Winnipeg, MB R3E 3M4, Canada. Phone: (204) 789-2027. Fax: (204) 789-2027. E. mail: hweingartl@inspection.gc.ca.

The aim of this work was to study the spread of Nipah virus isolated from a human encephalitis case in a porcine host during the first week postinfection, with focus on a route of central nervous system (CNS) invasion.

Neurotropic viruses can invade the central nervous system by two different routes, via peripheral nerves or hematogenously, using different mechanisms. Primary sensory neurons or motor neurons of the spinal cord for example, can provide a direct route to the CNS (27). Blood-borne viruses can use several ways to infect the CNS, although high-titer viremia is usually a prerequisite (20). One way is by virus entering the stroma of the choroid plexus through the fenestrated capillary endothelium from the blood, and than either infect or be passively transported across the choroid plexus epithelial cells into the CSF. From there the virus can infect the ependymal cells lining the walls of the ventricules and then invade the underlaying brain tissues (27). Another way is by direct infection or passive transport across the brain microvascular endothelial cells (11, 27). The third way is either by transmigration of activated infected T lymphocytes into the brain or by infected monocytes recruited by the lymphocytes (17). Factors increasing vascular permeability, such as specific cytokines, can also facilitate virus entry into brain, for example, tumor necrosis factor alpha in the case of human immunodeficiency virus invasion of the CNS (5).

Our study presents novel data indicating that Nipah virus can, following initial replication in the upper respiratory tract, invade the central nervous system directly via infected cranial nerves and by crossing the blood-brain barrier, possibly employing several mechanisms. Our findings on the neurotropism of Nipah virus in experimentally infected weaned piglets may have implications for understanding Nipah virus neurotropism also in other host species.

MATERIALS AND METHODS

Cells. African green monkey epithelial kidney (Vero 76) and porcine turbinate (PT-K 75) cells, obtained from the American Type Culture Collection (ATCC), were grown in Dulbecco's modified Eagle's medium/10% fetal bovine serum/100 IU penicillin/streptomycin/4 mM L-glutamine (WISENT)/10 mM HEPES (Sigma, St. Louis, MO)/1 mM sodium pyruvate (Gibco, Invitrogen, Grand Island, NY).

Virus. The human isolate of Nipah virus (passage 2 in Vero cells) was kindly provided by Thomas Ksiazek and Pierre Rollin, Centers for Disease Control, Atlanta. Virus stock for the animal experiments was prepared in PT-K75 monolayers in T75 flasks (Costar, Corning Inc., Corning, NY), infected with Nipah virus at a multiplicity of infection of 0.1 and incubated at 33°C for 72 h, when 80% cytopathic effect was reached. Virus was harvested by cell freeze-thaw, including supernatant, and clarified at 2,000 × g (4°C, 20 min). The titer of the virus stock was $10^{7.0}$ PFU/ml on PT-K75 cells and $10^{7.1}$ PFU/ml on Vero 76 cells.

Virus plaque assay. The virus plaque assay was performed in 12-well plates (Costar, Corning, NY) with either Vero 76 or PT-K75 confluent monolayers. Virus inoculum (400 μl/well) was incubated on cells for 1 h at 33°C, 5% CO_2 and then replaced with 2 ml of 2% carboxymethylcellulose, sodium salt, medium viscosity/Dulbecco's modified Eagle's medium (Sigma Chemical, St. Louis, MO)/2% fetal bovine serum overlay, and incubated at 33°C, 5% CO_2. The cells were fixed after 5 days with 4% formaldehyde and stained with 0.5% of crystal violet/80% methanol/phosphate-buffered saline (PBS).

Animals. Four-week-old crossbred Landrace female pigs were obtained from a high-health-status herd (Sunnyside Colony Ltd.), and acclimatized for 1 week prior to inoculation.

Based on serology, the herd is certified to be free of porcine reproductive and respiratory syndrome virus, *Mycoplasma hyopneumoniae*, swine influenza virus, *Actinobacillus pleuropneumoniae*, transmissible gastroenteritis virus, swine dysentery, mange, and lice.

Animal housing under biosafety level 4 conditions and all animal manipulations were approved by the Animal Care Committee of the Canadian Science Centre for Human and Animal Health, meeting the Canadian Council on Animal Care guidelines.

Experimental design. All animals were sampled prior to the inoculation, and monitored for clinical signs and body temperature changes during the experiment. Three control pigs (22, 23, 24), mock inoculated with PBS, were housed separately from the challenge pigs, and sampled the same way as the infected pigs.

The experiment was performed in two consecutive trials: trial one (pig 1 to 6); trial two (pig 16 to 21). During the acclimatization period, piglet 16 suffered an injury and was euthanized immediately prior to virus inoculation. The pigs were inoculated intranasally, orally and ocularly with total of 2.5×10^5 PFU per pig by dropping 0.25 ml of inoculum into each eye, placing approximately 1 ml into each nostril, and 1 ml into the throat. Each trial group was divided into two subgroups: 1A: pigs 4, 5, 6; 1B: pigs 1, 2, 3; 2A: pigs 17 and 18; and 2B**:** pigs 19, 20, 21. Subgroups A and B were sampled on alternate days starting at 2 days postinoculation to decrease the stress from anesthesia. Sampling was done under anaesthesia (medetomidine,60 μg/kg; ketamine, 20 mg/kg, *i.m.*), reversed with 2 of the volume of Atimepazole (5 mg/ml) after the sampling was finished. One pig a day was euthanized for tissue sample collection by exsanguination under deep anesthesia with 250 to 375 mg of sodium thiopental (Pentothal), followed by the administration of Euthanol, at 3 dpi (pigs 3 and 21), 4 dpi (pigs 6 and 18), 5 dpi (pigs 2 and 20), 6 dpi (pigs 5 and 17), 7 dpi (pigs 1 and 19), and 8 dpi (pig 4).

Sample collection. Blood from the right cranial vena cava was collected into sodium citrate tubes for virus isolation and reverse transcription (RT)-PCR, serum separator tubes (BD, Franklin Lakes, NJ) for serology, and CPT cell preparation tubes (BD, Franklin Lakes, NJ) to harvest peripheral mononuclear cells (PMBC) and plasma, according to the manufacturer's instruction. PMBC samples were harvested from serial bleeds during the first trial and in final bleeds of the second trial. Nasal, pharyngeal, ocular, and rectal swabs were collected for virus isolation and RT-PCR on the same days as blood. Polyester fiber swabs (BD, Sparks, MD) were emerged into 2 ml of PBS supplemented with PenStrep. After euthanasia, urine and the following tissues were collected for virus isolation, RT-PCR and pathology: hindbrain, forebrain, trigeminal ganglion, nasal turbinates, thymus, tonsil, spleen, pancreas, kidney, bladder, uterus, ovary, lymph nodes (submandibular, bronchial, inguinal, mesenteric), bone marrow (rib), lung, trachea, thyroid, ileum, heart, skeletal muscle, and liver. Additional samples were collected in the second trial: CSF, conjunctival and retrobulbar lymphoid tissue, tongue, olfactory bulb, optic nerve, medulla oblongata, cerebellum, midbrain (pons, thalamus), basal ganglia, meninges (if sloughed off), bronchus, and jejunum.

Virus isolation. Virus isolation attempts from whole blood, serum/plasma, swabs, urine, and tissues were performed as a plaque assay on PT-K75 cell monolayers in 12-well plates (Costar, Corning Inc., Corning, NY) as described above.

The 10% wt/vol tissue homogenates were prepared in cold, Ca^{2+}- and Mg^{2+}-free Dulbecco's PBS (DPBS) (Sigma, St. Louis, MO) supplemented with 1% vol/vol Pen/Strep (Wisent) by homogenization, either in a closed plastic bag in a MiniMix blender (Interscience) for 30 sec at 9 strokes/sec, or in the MixerMill stainless steel homogenizer (Retsch) for 1 min at 30 Hz. The homogenized tissues were clarified by centrifugation (2,000 × g, 20 min). Tenfold dilutions in DPBS (400 μl/well) of the of the tissue supernatants, whole blood, plasma, swabs, and urine were screened for virus presence.

Prior to virus isolation from swabs, 500 μg/ml (final) of gentamicin was added to the diluent following removal of the swab. The sample was then incubated at room temperature for 1 h, and clarified at 1,550 × g for 10 min. The isolation was repeated for the samples with high virus titer, diluting the samples up to 10^{-6}. Positive virus isolation on RT-PCR negative samples was repeated without the overlay, with RT-PCR performed on the supernatant from cells showing cytopathic effect to determine whether it was due to Nipah virus replication.

The sensitivity of virus isolation was determined by spiking spleen tissue from one negative control pig with virus control prior to homogenization. No difference was observed in virus titer between the spiked tissue sample and the virus control.

RT-PCR. Total RNA was extracted from 100 μl of the samples prepared for virus isolation by using TriPure Reagent (Roche Diagnostic Corporation, Indianapolis, IN) as per the manufacturer's instructions.

Two sets of primers were used in a one-step RT-PCR assay employing the QIAGEN OneStep RT-PCR kit (QIAGEN): forward primer ACA AGA AAA TAC AAG ATT AA and reverse primer TTC TTC ATT GCC TCA TATA, located within the F gene, yielding a 292-bp amplicon; and forward primer GCA CTT GAT GTG ATT AGA and reverse primer GGC AGT GTC GGG AGC TGT AA, located within the N gene, yielding a 395-bp amplicon.

The RT-PCR conditions were 30 min at 50°C and 15 min at 95°C, followed by 30 cycles of 95°C 30 sec, 50°C 30 sec, and 72°C 30 sec, and completed at 72°C for 10 min.

RT-PCR using the F primers detected viral RNA in samples containing approximately an equivalent of 10^{-1} PFU per 100 μl of sample, N primer set was about one log more sensitive than the F primer set.

Real time RT-PCR was performed on serum/plasma and PMBC samples only, according to Guillaume and others (8), using a SmartCycler (Cepheid), Quantitech kit (QIAGEN), and primers and probe (Applied Biosystems International) located within the N gene. The real time RT-PCR was standardized using Nipah virus N gene cloned in to the pSHAME2a plasmid, kindly provided by R. Bremner, University of Toronto, with sensitivity of 300 copies/reaction in 100 μl sample. Samples becoming positive at 35 cycles were considered negative. The N gene fragment copy numbers (plasmid standard) were related to PFU from five different Nipah virus stocks. In the three Vero cell-derived stocks, 1 PFU corresponded to 9,600, 16,100, and 10,500 copies, respectively, while in the PT-K75 cells derived stock 1 PFU corresponded to 761,500 copies.

Guinea pigs polyclonal serum. Two guinea pigs (500 g Hartley females, Charles River) housed in microisolator cages under biosafety level 4 conditions, were inoculated intraperitoneally with 2.5×10^5 PFU of live Nipah virus per guinea pig. Guinea pigs were boosted at 14 dpi with the same amount of live virus as for the first inoculation, and euthanized on 28 dpi by exsanguination under anesthesia (ketamine, 50 mg/kg and Xylazine, 10 mg/kg). Neutralizing antibody titers in the guinea pig sera were determined by microtiter plaque reduction neutralization assay (22). Serum dilutions causing 70% reduction of virus plaques were considered antibody positive.

Mouse monoclonal antibodies against Nipah N protein. Mouse monoclonal antibodies were raised by immunization with binary ethyneimine inactivated Nipah virus using standard hybridoma techniques. A mixture of the monoclonal antibodies that reacted on Western blot with N protein were used for the immunohistochemistry.

Immunohistochemistry. Staining was performed using the Biogenex Super-Sensitive kit (BioGenex Laboratories). Formalin-fixed paraffin-embedded 5μ sections, melted for 1 h at 58°C were incubated for 10 min with 3% H_2O_2 at room temperature, rinsed in Milli-Q water for 1 minute, and incubated with primary antibody (guinea pig polyclonal antiserum diluted 1:800 or mix of mouse monoclonal antibodies against the N protein diluted 1:100) in Tris-buffered saline containing 0.1% Tween 80 (TBST, Dakopatts/Denmark) and 10% normal goat serum, for 48 h at 4°C. The sections were then incubated for 1 h with the biotinylated, ready-to-use multilink (in 10% normal goat serum), followed by 10 min incubation with a horseradish peroxidase-conjugated streptavidin complex, and developed with 3, 3′-diaminobenzidine chromogen system (DakoCytomation) for 10 min. Sections were washed in TBST twice for 10 min between the incubations. Slides were counterstained with hematoxylin. Control samples included Nipah-infected tissues incubated with secondary antibody only, tissues from noninfected control pigs and classical swine fever virus-infected pigs.

TABLE 1. Virus isolation and RT-PCR for pharyngeal swabs[a]

Pig no.	Result on dpi:						
	2	3	4	5	6	7	8
3		+					
21		+					
6	−		−				
18	(+)		1.1				
2		−		3.0			
20		(+)		+			
5	−		+		−		
17	−		+		−		
1		−		−		−	
19		+		+		+	
4	−		−		−		−

[a] —, samples negative on both RT-PCR and virus isolation. +, samples negative on virus isolation but positive on RT-PCR using both set of primers. (+), samples positive on RT-PCR only with a primer set located in the N gene. The numbers indicate $\log_{10}$ PFU of virus isolated per ml of swab. These samples were also positive on RT-PCR.

TABLE 2. Virus isolation and RT-PCR for nasal swabs[a]

Pig no.	Result on dpi:						
	2	3	4	5	6	7	8
3		1.3					
21		(+)					
6	−		−				
18	(+)		+				
2		−		1.7			
20		+		+			
5	−		3.9		2.5		
17	+		1.1		+		
1		−		−		+	
19		1.1		+		1.4	
4	−		−		+		−

[a] See Table 1; footnote *a*.

RESULTS

Clinical signs. Pig 2 showed neurological signs on day 5 postinoculation (wide stance, difficulty standing, unsteady balance causing the animal to back up, restless) and was euthanized on the same day. Pig 19 showed neurological signs on 7 dpi (lethargic, not willing to walk, standing in sawhorse stance, depressed with head down and ears back, suffering with severe shivering and seizures upon stimulus) and was euthanized the same day. The remaining nine infected pigs were clinically healthy until the end of the experiment (up to 8 dpi). The rectal temperatures for all pigs, with the exception of one, remained stable within the normal range (39.0 to 39.3°C). Pig 4 had increased rectal temperature of 40.5°C at 6dpi and 41.3°C at 8 dpi, still below the guidelines for administration of antipyretics. Mock-inoculated control pigs displayed no clinical signs.

Virus isolation. Infectious virus was first detected in nasal swabs at 3 dpi and in the pharyngeal swabs starting at 4 dpi (Tables 1, 2, and 3). No infectious virus was isolated from the ocular and rectal swabs, whole blood, urine, or serum/plasma in course of this experiment.

Table 4 summarizes tissues which yielded infectious virus. Virus was isolated from the upper respiratory tract (nasal turbinates and trachea) in six out of eight pigs, and submandibular lymph nodes at 3 dpi (first time point for tissue sample collection). Starting from day 4 postinfection, virus was isolated also from the lower respiratory tract (lungs and bronchus) in four out of eight pigs. Infectious virus was not detected in the respiratory tract of pig 4, including the swabs. Additional lym-

TABLE 3. Results of real-time RT-PCR for white blood cells and plasma and serum samples and of RT-PCR for ocular swabs

dpi	No. of animals positive/no. tested		
	Ocular swab	White blood cells	Plasma/serum
2	2/5	1/3	2/5
3	3/6	1/3	3/6
4	2/5	0/3	4/5
5	1/4	1/2	1/4
6	1/3	0/2	2/3
7	1/2	0/1	2/2
8	0/1	0/1	1/1

TABLE 4. Virus isolation and RT-PCR of tissues[a]

Sample	Result on dpi for pig no.:										
	3 dpi		4 dpi		5 dpi		6 dpi		7 dpi		8 dpi, 4
	3	21	6	18	2	20	5	17	1	19	
Hindbrain	−		−		7.7		−		−		+
Forebrain	−		−		6.9		−		−		+
Trigeminal ganglion	−	−	−	−	2.1	2.4	5.5	−	2.1	3.3	+
Pons		+		+		+		−		4.3	
Thalamus		+		−		+		−		4.1	
Cerebellum		−		−		+		+		2.9	
Olfactory bulb		+		+		−		3.6		2.4	
Optic nerve		−		−		−		−		4.4	
Medulla oblongata		−		−		−		−		4.0	
Midbrain		−		−		3.3		−		4.0	
Basal ganglia		−		−		2.1		−		2.4	
Meninges		ND		−		ND		ND		4.4	
CSF		+		+		+		+		4.7	
Lung	−	−	−	2.1	2.8	−	−	3.4	2.4	−	−
Bronchus		−		4.4		−		+		−	
Trachea	3.5	+	3.4	+	5.2	2.4	−	3.3	−	3.7	−
Nasal turbinates	5.0	4.1	2.6	4.1	5.3	4.3	−	4.4	−	3.7	+
Tongue		−		2.1		2.1		2.6		−	
Submandibular lymph node	2.6	−	3.1	−	5.8	−	5.9	3.5	6.0	3.4	+
Bronchial lymph node	−	(+)	−	+	−	3.9	2.9	4.0	−	4.0	−
Conjuctival lymphoid tissue		+		+		+		+		+	
Retrobulbar lymphoid tissue		(+)		(+)		+		+		3.3	
Tonsil	−	−	−	−	−	−	−	−	−	4.3	−
Spleen	−	+	−	+	−	2.1	−	2.1	−	+	−

[a] See Table 1, footnote *a*.

phoid tissues (bronchial lymph nodes, retrobulbar lymphoid tissue, tonsil and spleen) yielded infectious virus starting at 5 dpi in four out of seven pigs. In the nervous system, Nipah virus was isolated from trigeminal ganglion starting at 5 dpi in five out of seven pigs. Starting at the same dpi, other nervous tissues yielded virus on virus isolation in six out of seven pigs, with the exception of pig 4 (8 dpi).

The following tissues were negative on virus isolation: liver, heart, kidney, thymus, pancreas, bone marrow (rib), bladder, uterus, ovary, conjuctival lymphoid tissue, inguinal and mesenteric lymph nodes, thyroid, ileum, jejunum, and skeletal muscle.

In summary, during the early phase of the infection, Nipah virus was isolated from respiratory, lymphatic and nervous systems.

RT-PCR (classical and real time). Ocular, pharyngeal and nasal swabs tested positive for Nipah virus RNA starting at 2 dpi, either by both sets of primers located within the N and F genes, or with the N gene primers only. Tables 1 and 2 summarize the results of virus isolation and RT-PCR on nasal and pharyngeal swabs in individual animals at specific dpi. Table 3 summarizes the real-time RT-PCR results for PMBC, plasma/serum and the RT-PCR results for the ocular swabs by relating the number of positive animals to the number of tested animals. Weak viremia in plasma/serum (167,500 copies to 22,000 copies, representing a range from 17.5 to 2.3 PFU to 0.22 to 0.029 PFU, depending on virus stock used as a standard) was detected throughout the duration of the experiment, starting at 2 dpi using the real-time RT-PCR with primers and the probe located within the N gene. Presence of low levels of neutralizing antibodies, which could affect the attempts for virus isolation, cannot be excluded. Low content of viral RNA (22400 to 1950 copies, representing a range from 2.4 to 0.2 to 0.03 to 0.0026 PFU, depending on virus stock used as a standard) was detected in the PMBC fraction during the first trial in three animals (pigs 2, 4, and 5). The final bleeds for pigs 17 to 21 in the second trial tested negative, and not included in the Table 3. Pigs 3, 17, 18, and 20 remained without detectable viremia (serum or PMBC). Whole blood, urine and rectal swabs were negative on RT-PCR using the two primer sets, located in the N and F gene regions.

Results for detection of viral RNA on RT-PCR in tissues, which tested positive at least at one point during the experiment are summarized in Table 2. We were able to amplify Nipah virus RNA in the upper respiratory tract, and the lymphoid system as early as 2 dpi. Starting from 3 dpi, viral RNA was detected in the lungs and bronchus, and in the nervous system in nine out of eleven pigs. Although the RT-PCR is more sensitive than virus isolation we were able to detect viral RNA again only in the respiratory, lymphoreticular and nervous systems, and not in any other organs/tissues.

Immunohistochemistry. Nipah virus antigen was observed in the smooth muscle and endothelial cells of medium-to-large-size veins, and to a significantly lesser extent in the arteries of the central nervous, respiratory and lymphoid systems. Positive immunostaining in the cells of the vascular system was detected more frequently than in the infiltrating cells of the perivascular cuffs such as lymphocytes or monocytes/macrophages. Cells of the brain parenchyma including neurons/neuronal processes and glial cells, epithelial cells of the respiratory tract, and dendritic cells of the lymph nodes/spleen were positive for presence of viral antigen.

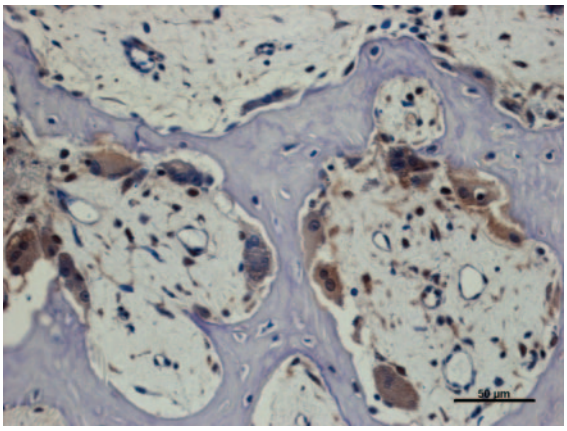

FIG. 1. Presence of Nipah virus antigen in the nasal turbinate. Positive staining in large multinucleate cells, consistent with osteoclasts, and smaller uninucleate cells (may be osteoclasts or osteoblasts) located along the margins of the bone trabeculae. Immunostaining using polyclonal guinea pig anti-Nipah virus serum. Pig 5, 6 dpi, nasal turbinate. Scale bar represents 50 μm.

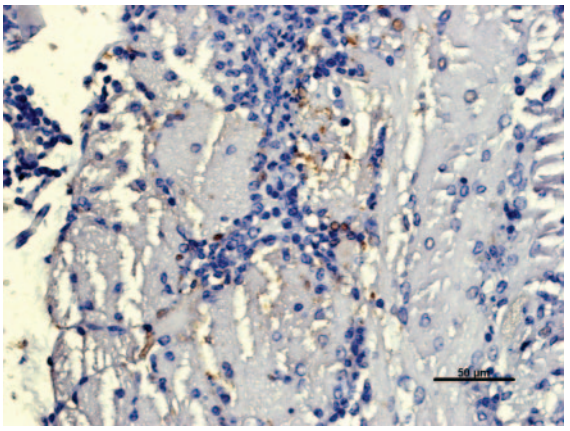

FIG. 3. Presence of Nipah virus antigen in the granule cell neurons of the olfactory bulb (secondary sensory neuron). Immunostaining using polyclonal guinea pig anti-Nipah virus serum. Animal 19, 7 dpi, olfactory bulb. Scale bar represents 50 μm.

In the respiratory tract, NV antigen was demonstrated mainly in the nasal turbinates and to a lower extent in trachea and lungs. Osteoclasts and possibly also osteoblasts in the nasal turbinate bone (Fig. 1), respiratory epithelial cells, and smooth muscle cells of the blood vessels in the nasal turbinates were infected, in addition to the filae olfactoriae (Fig. 2). Occasionally, infiltrating cells (lymphocytes, macrophages) were immunohistochemistry (IHC) positive for the antigen (pig 18 at 4 dpi). Infection of the trachea was detected in 2 animals at 4 and 7 dpi, respectively (18, 19), and was confined to the epithelial cells (18) and/or multinucleated giant cells and infiltrating cells within the submucosa (pigs 18 and 19). The same immunostaining pattern was observed within the lungs where first staining was observed at 3 dpi within blood vessel walls (pig 3), at 4 dpi in the epithelial cells of bronchioli, in the inflammatory and multinucleated giant cells within the interstitium (pigs 6 and 18) and persisted until the termination of the experiment (pigs 5 and 19).

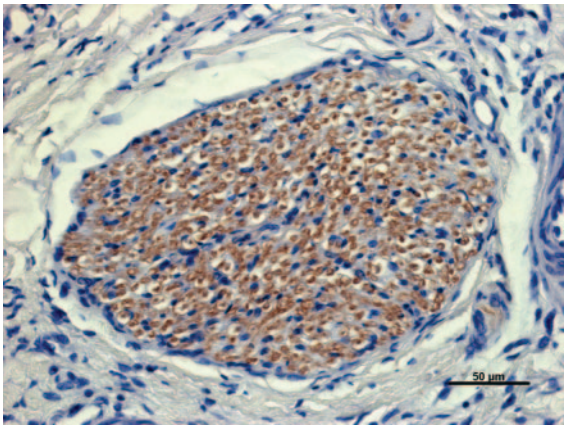

FIG. 2. Positive immunostaining for Nipah virus antigen of the axons on the cross-section of the olfactory nerve in the turbinates. Positive staining of the Schwann's cells was not observed on the sections. Immunostaining using polyclonal guinea pig anti-Nipah virus serum. Pig 5, 6 dpi, nasal turbinate. Scale bar represents 50 μm.

Distribution of the Nipah virus antigen in the lymphoid system was restricted mainly to the submandibular lymph nodes. The submandibular lymph nodes were always IHC positive, namely the endothelial cells of blood/lymphatic vessels, multinucleated giant cells (pig 4) and follicular dendritic cells, characterized by their location and long filamentous cell processes. In two animals (pigs 5 and 19) at 6 and 7 dpi, respectively, IHC staining was also found in bronchial lymph nodes with a cellular distribution similar to the submandibular lymph node. In one animal (pig 19), Nipah virus antigen was detected in the spleen in endothelial cells of blood/lymphatic vessels and in follicular dendritic cells.

Nipah virus antigen was consistently detected in the cranial nerves. It was detected in the filae of the olfactory nerve for the duration of the experiment, starting at 3 dpi. (Fig. 2) Positive immunostaining for Nipah virus antigen was detected in the axons of the olfactory and trigeminal nerves. The hypoglossal and the glossopharygeal nerves within the tongue were IHC positive in pig 17 at 6 dpi. Fibers of the autonomic nerves in trachea and esophagus, and also of the spinal nerve in the *musculus longissimus lumborum* were found to be infected at 8 dpi in pig 4.

Viral antigen was detected in the granular cells of the olfactory bulb of pig 19 (7 dpi) (Fig. 3), indicating that the virus entered the brain via the olfactory pathways. Nipah virus antigen was also located at the outer (leptomeninges) and inner surfaces (ventricle lining and ependyma) of the brain in the same animal. At 5 dpi, Nipah virus antigen was detected in the inner surface of the brain-ventricle ependyma and choroid plexus stroma of animal No 2 and 20 (Fig. 4). Positive staining in the endothelial and smooth muscle cells of meningeal veins was detected at 5, 6, and 7 dpi (pigs 2, 5, and 19, respectively), and a day earlier in the veins of the cerebral cortex of pig 6 (4 dpi) (Fig. 5). In the animals with neurological signs (pigs 2 and 19), the viral antigen was observed in the brain cells at 5 and 7 dpi, respectively. That included neurons and glial cells (astro-

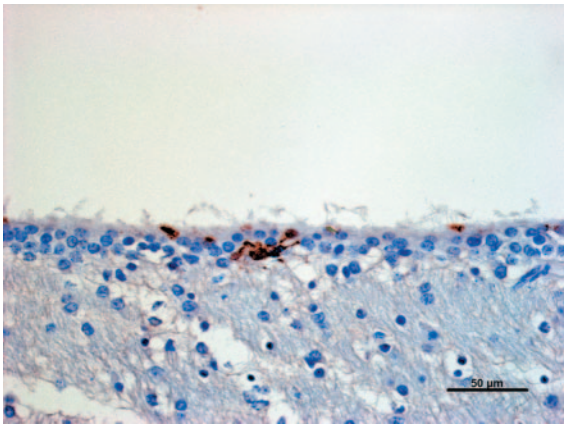

FIG. 4. Positive immunostaining for Nipah virus N protein using mouse monoclonal anti-N antibodies in the ependymal lining of the third ventricle. Pig 5, 6 dpi. Scale bar represents 50 μm.

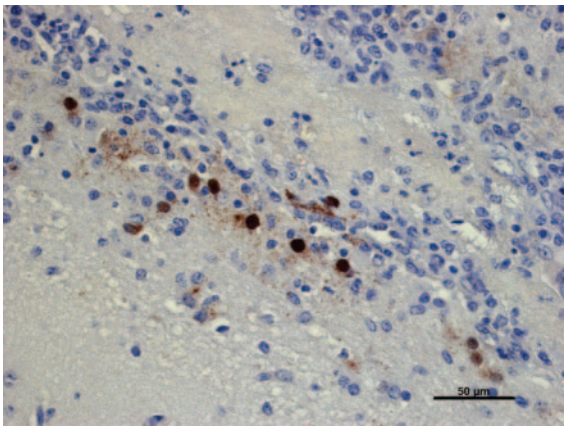

FIG. 6. Positive immunostaining for Nipah virus N protein, using mouse monoclonal anti-N antibodies, in brain cells, mainly in glia cells and occasionally neurons in an animal with fulminant virus-induced meningitis. Animal 19, 7 dpi, cerebral cortex. Scale bar represents 50 μm.

cytes, microglia) in the most superficial layers (I and II) of the cerebral cortex and the olfactory bulb (Fig. 6).

Corresponding negative control tissue samples from PBS-inoculated pigs and from pigs infected with classical swine fever virus were included to address possibility of nonspecific staining. In addition the tissues sections were probed with both guinea pig polyclonal anti-Nipah virus serum and with mouse anti-Nipah virus N protein monoclonal antibodies. The immunohistochemistry results strongly supported results generated by virus isolation and/or RT-PCR.

DISCUSSION

The data presented in this study indicate for the first time that Nipah virus can invade the CNS of a porcine host directly via the cranial nerves and by crossing the blood-brain barrier, as suggested for another porcine paramyxovirus (*Rubulavirus* La Piedad-Michoacan virus) (13, 18).

In the experimentally inoculated animals, Nipah virus initially replicated in the oronasal cavity. Virus was detected in the nasal swabs as early as 2 dpi and a day later also in the pharyngeal swabs. The early virus isolation from nasal turbinates, trachea, and especially from the submandibular lymph nodes (submandibular lymph nodes drain the anterior nasal cavity) at 3 dpi supported the findings.

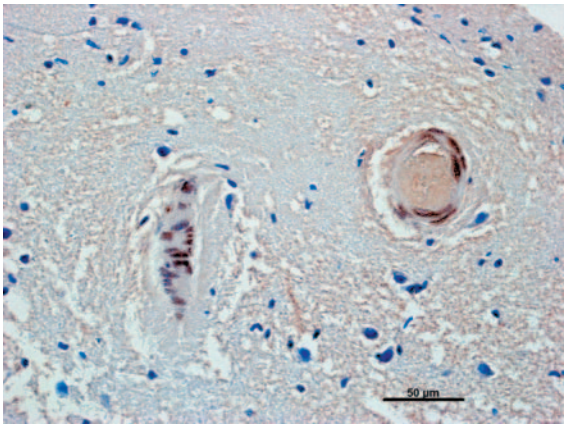

FIG. 5. Nipah virus antigen detected in the smooth muscle cells and in the endothelial cells of small blood vessels in the brain using polyclonal guinea pig anti-Nipah virus serum. Pig 5, 6 dpi, cerebral cortex. Scale bar represents 50 μm.

It appears that the virus infected the olfactory and respiratory epithelial cells, cranial nerves, and cells of the immune system (lymphocytes, macrophages, and monocytes), initiating viremia (both cell associated and free) and spreading further in the reticuloendothelial system, with additional replication in endothelial cells of the blood/lymphatic vessels and spilling over into the smooth muscle cells of the blood vessels. Nipah virus appeared to move into the central nervous system via the cranial nerves, most importantly via the olfactory nerve, which was positive on IHC and RT-PCR at 3 dpi, followed by positive axonal staining in the trigeminal nerve. Starting at 5 dpi, virus was detected consistently (six out of seven animals) in the trigeminal ganglion either by virus isolation or RT-PCR. The hypoglossal and glossopharyngeal nerves were positive for viral antigen by IHC at 6 dpi and the optic nerve on day 7 postinoculation by virus isolation. It cannot be excluded that at the later dpi an anterograde dissemination of the virus takes place.

Nipah virus likely reached the CNS also by crossing the blood-brain barrier, although a hematogenous route of CNS invasion appears to be less important then the direct nervous system route. The real-time RT-PCR results indicated the presence of the virus in the blood, but the failure to isolate the virus on the original attempts suggested only a low level of viremia. Positive immunostaining of lymphocytes and monocytes/macrophages, and especially osteoclasts, indirectly indicated the presence of viremia. The virus possibly exploits several pathways of crossing the blood-brain barrier. It could cross via the choroid plexus, as supported by the positive IHC staining of the choroid plexus stroma and the ependymal lining of the ventricules and the detection of the virus in the CSF. Additionally, replication of the virus in the endothelial cells of the blood vessels in the brain and the resident brain cells in the proximity of the infected blood vessels could have facilitated virus crossover into the parenchyma of the CNS. Virus entry

into the brain by transmigration of infected cells cannot be excluded, as a number of antigen-positive lymphocytes and monocytes/macrophages were observed in the vicinity of blood and lymphatic vessels. As almost no histopathological changes in blood vessels were observed, damage to the walls of the blood vessels may not be a likely way of virus entry into the brain.

Concurrently, with the spread through the nervous and lymphoreticular systems, Nipah virus also replicated in the respiratory system, reaching the trachea through the pharynx and the rest of the respiratory tract, including the lung. Nasal shedding was detected in all pigs at least at one point during the infection and could possibly be used for noninvasive sampling for virus detection.

Despite the lack of respiratory signs early postinfection, as observed also by others (14, 10), our data confirm that the respiratory tract is one of the main virus targets early in the infection, with the nasal cavity as an entry and replication site for the virus. The nasal route of initiation of infection may be specific to pigs, also due to their behavior patterns (rooting and food sniffing).

Several members of the family *Paramyxoviridae* invade the CNS. Crossing of the blood-brain barrier as a route of CNS invasion has been suggested for measles (6), mumps (2), Hendra (23), and canine distemper (12) viruses. The only paramyxovirus presumed to access the CNS directly via the axons following intranasal exposure is the porcine rubulavirus La Piedad-Michoacan virus (18). In the case of other neurotropic paramyxoviruses such as phocine distemper virus, dolphin and porpoise morbillivirus (7), and velogenic neurotropic Newcastle disease virus (1), the route of CNS invasion was not proposed.

This work provided supporting data for Nipah virus entry into the CNS by crossing the blood-brain barrier, as previously suggested for human infections (25), and in addition provided novel data indicating direct infection of the CNS via peripheral nerves. The consistently rapid Nipah virus neuroinvasion in all inoculated animals in this study compared to the previously published data may reflect the type of virus isolate, pig breed, and quite importantly the route of ocular and oronasal inoculation versus subcutaneous or oral inoculation (14, 10). Nipah virus appears to be neuroinvasive in young pigs, and it remains to be determined whether that is the case also in older pigs. The relationship between neurotropism and neurovirulence is an interesting question for further investigations, as it may vary in different host species.

ACKNOWLEDGMENTS

This work was supported by Canadian Food Inspection Agency technical development grant TD W0207 fund and by Department of National Defense CRTI grant RD 0196.

We thank John Muschialli, AAHL, CSIRO, for his contribution to the biosafety level 4 animal work.

REFERENCES

1. **Brown, C., D. J. King, and B. S. Seal.** 1999. Pathogenesis of Newcastle disease in chickens experimentally infected with viruses of different virulence. Vet. Pathol. **36:**125–132.
2. **Carbone, K. M., and J. S. Wolinsky.** 2001. Mumps virus, p. 1381–1400. *In* D. M. Knipe and P. M. Howley (ed.), Fields virology, 4th ed. Lippincott Williams and Wilkins, Philadelphia, Pa.
3. **Chua, K. B., W. J. Bellini, P. A. Rota, B. H. Harcourt, A. Tamin, S. K. Lam, T. G. Ksiazek, P. E. Rollin, S. R. Zaki, W.-J. Shieh, C. S. Goldsmith, D. J. Gubler, J. T. Roehring, B. Eaton, A. R. Gould, J. Olson, H. Field, P. Daniels, A. E. Ling, C. J. Peters, L. J. Anderson, and B. W. J. Mahy.** 2000. Nipah virus: a recently emergent deadly paramyxovirus. Science **288:**1432–1435.
4. **Chua, K. B.** 2003. Nipah virus outbreak in Malaysia. J. Clin. Virol. **26:**265–275.
5. **Fiala, M., D. J. Looney, M. Stins, D. D. Way, L. Zhang, X. Gan, F. Chiappelli, E. S. Schweitzer, P. Shapshak, M. Weinand, M. C. Graves, M. Witte, and K. S. Kim.** 1997. TNF-alpha opens a paracellular route for HIV-1 invasion across the blood-brain barrier. Mol. Med. **3:**553–564.
6. **Griffin, D. E.** 2001. Measles virus, p. 1401–1441 *In* D. M. Knipe and P. M. Howley (ed.), Fields virology, 4th ed. Lippincott Williams and Wilkins, Philadelphia, Pa.
7. **Griot, C., M. Vandevelde, M. Schobesberger, and A. Zurbriggen.** 2003. Canine distemper, a re-emerging morbillivirus with complex neuropathogenic mechanism. Anim. Health Res. Rev. **4:**1–10.
8. **Guillaume, V., A. Lefeuvre, C. Faure, P. Marianneau, R. Buckland, S. K. Lam, T. F. Wild, and V. Deubel.** 2004. Specific detection of Nipah virus using real-time RT-PCR (TaqMan). J. Virol. Methods **120:**229–237.
9. **Harcourt, B. H., A. Tamin, K. Halpin, T. G. Ksiazek, P. E. Rollin, W. J. Bellini, and P. A. Rota.** 2001. Molecular characterization of the polymerase gene and genomic termini of Nipah virus. Virology **287:**192–201.
10. **Hooper, P., S. Zaki, P. Daniels, and D. Middleton.** 2001. Comparative pathology of the diseases caused by Hendra and Nipah viruses. Microb. Infect. **3:**315–322.
11. **Huang, S. H., and A. Y. Jong.** 2001. Cellular mechanisms of microbial proteins contributing to invasion of the blood-brain barrier. Cell Microbiol. **3:**277–287.
12. **Krakowka, S., L. C. Cork, J. A. Winkelstein, and M. K. Axthelm.** 1987. Establishment of central nervous system infection by canine distemper virus: breach of the blood-brain barrier and facilitation by antiviral antibody. Vet. Immunol. Immunopathol. **17:**471–482.
13. **Mendoza-Magaña, M. L., M. A. Ramírez-Herrera, J. M. Dueñas-Jiménez, and S. H. Dueñas-Jiménez.** 2001. Pig paramyxovirus of the blue eye disease binding to a 116kDa glycoprotein expressed in pig neuronal membranes. J. Vet. Med. B **48:**489–499.
14. **Middleton, D. J., H. A. Westbury, C. J. Morrissy, B. M. van der Heide, G. M. Russel, M. A. Braun, and A. D. Hyatt.** 2002. Experimental Nipah virus infection in pigs and cats. J. Comp. Pathol. **126:**124–136.
15. **Mohd Nor, M. N., C. H. Gan, and B. L. Ong.** 2000. Nipah virus infection of pigs in peninsular Malaysia. Rev. Sci. Tech. Off. Int. Epizoot. **19:**160–165.
16. **Murray, K., R. Rogers, L. Selvey, P. Selleck, A. Hyatt, A. Gould, L. Gleeson, P. Hooper, and H. Westbury.** 1995. A novel morbillivirus pneumonia of horses and its transmission to humans. Emerg. Infect. Dis. **1:**31–33.
17. **Pachter, J. S., H. E. de Vries, and Z. Fabry.** 2003. The blood-brain barrier and its role in immune privilege in the central nervous system. J. Neuropathol. Exp. Neurol. **62:**593–604.
18. **Stephano, H. A.** 1999. Blue eye disease, p. 103–112. *In* B. E. Straw, S. D'Allaire, W. L. Mengeling, and D. J. Taylor (ed.), Diseases of swine, 8th ed. Blackwell Science, Oxford, United Kingdom.
19. **Tanimura, N., T. Imada, Y. Kashiwazaki, S. Shahirudin, S. H. Sharifah, and A. J. Aziz.** 2004. Monoclonal antibody-based immunohistochemical diagnosis of Malaysian Nipah virus infection in pigs. J. Comp. Pathol. **131:**199–206.
20. **Tyler, K. L., and N. Nathanson.** 2001. Pathogenesis of viral infections, p. 199–244, *In* D. M. Knipe and P. M. Howley (ed.), Fields virology, 4th ed. Lippincott Williams and Wilkins, Philadelphia, Pa.
21. **Wang, L. F., B. H. Harcourt, M. Yu, A. Tamin, P. A. Rota, W. J. Bellini, and B. T. Eaton.** 2001. Microbes Infect. **3:**279–287.
22. **Weingartl, H. M., M. A. Drebot, Z. Hubalek, J. Halouzka, M. Andonova, A. Dibernardo, C. Cottam-Birt, J. Larence, and P. Marszal.** 2003. Comparison of assays for the detection of West Nile virus antibodies in chicken serum. Can. J. Vet. Res. **67:**128–132.
23. **Williamson, M. M., P. T. Hooper, P. W. Selleck, H. A. Westbury, and R. F. S. Slocombe.** 2001. A guinea-pig model of Hendra virus encephalitis. J. Comp. Pathol. **124:**273–279.
24. **Wong, K. T., W. J. Shieh, S. R. Zaki, and C. T. Tan.** 2002. Nipah virus infection, and emerging paramyxoviral zoonosis. Springer Semin. Immunopathol. **24:**215–228.
25. **Wong, K. T., W. J. Shieh, S. Kumar, K. Norain, W. Abdullah, J. Guarner, C. S. Goldsmith, K. B. Chua, S. K. Lam, C. T. Tan, K. J. Goh, H. T. Chong, R. Jusoh, P. E. Rollin, T. G. Ksiazek, S. R. Zaki, and Nipah Virus Pathology Working Group.** 2002. Nipah virus infection: pathology and pathogenesis of an emerging paramyxoviral zoonosis. Am. J. Pathol. **161:**2153–2167.
26. **Yu, M., E. Hansson, B. Shiell, W. Michalski, B. T. Eaton, and L. F. Wang.** 1998. Sequence analysis of the Hendra virus nucleoprotein gene: comparison with other members of the subfamily Paramyxovirinae. J. Gen. Virol. **79:**1775–1780.
27. **Zhang, J. R., and E. Tuomanen.** 1999. Molecular and cellular mechanisms for microbial entry into the CNS. J. Neurovirol. **5:**591–603.